



The long non-coding RNA PFI protects against pulmonary fibrosis by interacting with splicing regulator SRSF1

Jian Sun^{1,2} · Tongzhu Jin^{1,2} · Wei Su^{1,2} · Yingying Guo^{1,2} · Zhihui Niu^{1,2} · Jiayu Guo^{1,2} · Liangliang Li^{1,2} · Jiayi Wang^{1,2} · Lu Ma^{1,2} · Tong Yu^{1,2} · Xuelian Li¹ · Yuhong Zhou¹ · Hongli Shan^{1,2,3} · Haihai Liang^{1,2,3}

Received: 6 November 2020 / Revised: 17 April 2021 / Accepted: 21 April 2021 / Published online: 12 May 2021
© The Author(s), under exclusive licence to ADMC Associazione Differenziamento e Morte Cellulare 2021

Abstract

Pulmonary fibrosis (PF) is a type of interstitial pneumonia with complex etiology and high mortality, characterized by progressive scarring of the alveolar interstitium and myofibroblastic lesions. Recently, there has been growing appreciation of the importance of long non-coding RNAs (lncRNAs) in organ fibrosis. The aim of this study was to investigate the role of lncRNAs in lung fibrosis. We used a qRT-PCR assay to identify dysregulated lncRNAs in the lungs of mice with experimental, bleomycin (BLM)-induced pulmonary fibrosis, and a series of molecular assays to assess the role of the novel lncRNA NONMMUT060091, designated as pulmonary fibrosis inhibitor (PFI), which was significantly downregulated in lung fibrosis. Functionally, knockdown of endogenous PFI by smart silencer promoted proliferation, differentiation, and extracellular matrix (ECM) deposition in primary mouse lung fibroblasts (MLFs). In contrast, overexpression of PFI partially abrogated TGF- β 1-induced fibrogenesis both in MLFs and in the human fetal lung fibroblast MRC-5 cells. Similarly, PFI overexpression attenuated BLM-induced pulmonary fibrosis compared with wild type (WT) mice. Mechanistically, using chromatin isolation by RNA purification-mass spectrometry (ChIRP-MS) and an RNA pull-down assay, PFI was found to directly bind Serine/arginine-rich splicing factor 1 (SRSF1), and to repress its expression and pro-fibrotic activity. Furthermore, silencing of SRSF1 inhibited TGF- β 1-induced proliferation, differentiation, and ECM deposition in MRC-5 cells by limiting the formation of the EDA+Fn1 splicing isoform; whereas forced expression of SRSF1 by intratracheal injection of adeno-associated virus 5 (AAV5) ablated the anti-fibrotic effect of PFI in BLM-treated mice. Overall, these data reveal that PFI mitigated pulmonary fibrosis through negative regulation of the expression and activity of SRSF1 to decrease the formation of the EDA+Fn1 splicing isoform, and suggest that PFI and SRSF1 may serve as potential targets for the treatment of lung fibrosis.

These authors contributed equally: Jian Sun, Tongzhu Jin, Wei Su.

Edited by H. Ichijo

Supplementary information The online version contains supplementary material available at <https://doi.org/10.1038/s41418-021-00792-1>.

✉ Hongli Shan
shanhongli@ems.hrbmu.edu.cn

✉ Haihai Liang
lianghaihai@ems.hrbmu.edu.cn

¹ Department of Pharmacology (State-Province Key Laboratories of Biomedicine-Pharmaceutics of China, Key Laboratory of Cardiovascular Research, Ministry of Education), College of

Introduction

Pulmonary fibrosis (PF) is a progressive, irreversible chronic inflammatory disorder, strongly age-related and with limited therapeutic options [1, 2]. It mainly includes idiopathic pulmonary fibrosis (IPF), allergic pneumonia, pneumoconiosis, sarcoidosis, and fibrogenic alveolitis related to collagen deposition. These forms of PF are caused by different stimulating factors such as poison, infection, severe trauma,

Pharmacy, Harbin Medical University, Harbin, Heilongjiang, P. R. China

² Northern Translational Medicine Research and Cooperation Center, Heilongjiang Academy of Medical Sciences, Harbin Medical University, Harbin, Heilongjiang, P. R. China

³ Research Unit of Noninfectious Chronic Diseases in Frigid Zone (2019RU070), Chinese Academy of Medical Sciences, Harbin, Heilongjiang, P. R. China

autoimmune reaction, and adverse drug reactions [3–5]. Cell senescence, epigenetic regulation, and environmental factors may cause PF [6–8], but the corresponding specific mechanisms have not been elucidated. Previous studies have shown that the main pathophysiological features in the process of PF include alveolar epithelial cells injury, abnormal activation of fibroblasts, and excessive deposition of extracellular matrix (ECM), eventually leading to respiratory failure and loss of pulmonary gas exchange function [9, 10]. Although the antifibrotic drugs pirfenidone and nintedanib have been approved for the clinical treatment of IPF, their toxicity and poor prognosis make this disease an open and urgent medical problem [11–13]. Therefore, it is particularly important to further explore the pathogenesis of PF, and to find novel targets for its diagnosis and treatment.

In recent years, a large number of studies have found that long non-coding RNAs (lncRNAs) are involved in the regulation of tissue repair and organ fibrosis, including cardiac fibrosis [14], hepatic fibrosis [15], renal fibrosis [16], and PF [17]. Yan et al. found that lncRNA MALAT1 regulates the expression of PI3K P85 through competitive binding with miR-503, thus accelerating the process of epithelial-to-mesenchymal transition (EMT) and promoting PF induced by silica [18]. Liu et al. found that lncRNA PCF promoted TGF- β 1-induced epithelial cell proliferation through competitive adsorption of miR-344-5p, while its silencing could significantly reduce PF in mice [19]. Our previous studies have revealed that lncRNA PFAR regulates the expression of YAP1/ Twist through competitive binding to miR-15a/miR-138, and participates in the regulation of IPF [20, 21].

In addition to endogenous competitive binding with microRNAs, lncRNAs also participate in the process of organ fibrosis through transcriptional regulation and epigenetic modifications. Hao et al. revealed that lncRNA SAFE combines with its adjacent gene *Sfrp2*, transcriptionally regulating the expression of its mRNA and thus playing an anti-fibrotic role [22]. Wang et al. found that lncRNA *NRON* reduces cardiac fibrosis by upregulating the phosphorylation level of the transcription factor NFATc3 [23]. The lncRNA *TSI*, moreover, targets the MH2 domain of the Smad3 protein, blocking its interaction with the TGF- β I receptor, thereby inhibiting the TGF- β /Smad signaling pathway and relieving renal fibrosis [24]. Taken together, these studies confirm that lncRNAs can also participate in the occurrence of organ fibrosis by regulating the activity of transcription factors, interacting with proteins, and interfering with the expression of adjacent genes.

Here, we identified a lncRNA, NONMMUT060091, with low expression in bleomycin (BLM)-induced PF, which we named pulmonary fibrosis inhibitor (PFI), and explored its function and mechanism in PF. Because of the mainly nuclear location of PFI, we hypothesized that it

could play a role in the process of lung fibrosis through binding to some proteins. Moreover, we aimed to determine whether it could be used as a nucleic acid drug to interfere with the progression of PF through exogenous administration, thus providing a novel strategy for the prevention and treatment of lung fibrosis.

Results

Inhibition of lncRNA PFI promotes fibrogenesis in primary mouse lung fibroblasts (MLFs)

First, we performed a qRT-PCR assay to examine the dysregulated lncRNAs in the lungs of mice with experimental, BLM-induced PF. As shown in Fig. 1A, six lncRNAs were upregulated, whereas two were downregulated in the lungs of BLM mice. Among the latter, we found that lncRNA NONMMUT060091, which we named PFI, was also markedly decreased in TGF- β 1-treated primary MLFs (Fig. 1B).

To examine whether PFI is involved in the process of PF, we constructed a smart silencer (SSi-PFI) to inhibit its endogenous expression in MLFs (Fig. 1C). qRT-PCR showed that PFI knockdown promoted the expression of collagen 1 α 1, collagen 3 α 1, Fn1, CTGF, and ACTA2 mRNAs in MLFs (Fig. 1D). At the same time, PFI inhibition resulted in the upregulation of Fn1, Collagen I, and α -SMA at the protein level compared with the negative control (SSi-NC) (Fig. 1E). Since abnormal activation of myofibroblasts and excessive proliferation of fibroblasts are the major causes of fibrosis, in order to fully reveal the mechanism by which PFI regulates PF, we further explored its possible involvement in the formation of myofibroblasts. As illustrated in Fig. 1F, PFI knockdown promoted the transition of fibroblasts into myofibroblasts. Moreover, we found that silencing PFI could significantly promote the proliferation of fibroblasts (Fig. 1G). We also used a wound healing assay to examine the effect of PFI on the migration ability of fibroblasts. As shown in Fig. 1H, PFI knockdown could significantly increase the ability of cells to migrate and promote wound healing.

Forced expression of lncRNA PFI attenuates TGF- β 1-induced fibrogenesis in MLFs

Next, we transfected PFI into TGF- β 1-treated MLFs to further determine its potential anti-fibrotic effect (Fig. 2A), the RNA sequences we used were shown in Supplemental Fig. 1. As expected, qRT-PCR showed that TGF- β 1 could significantly promote the mRNA

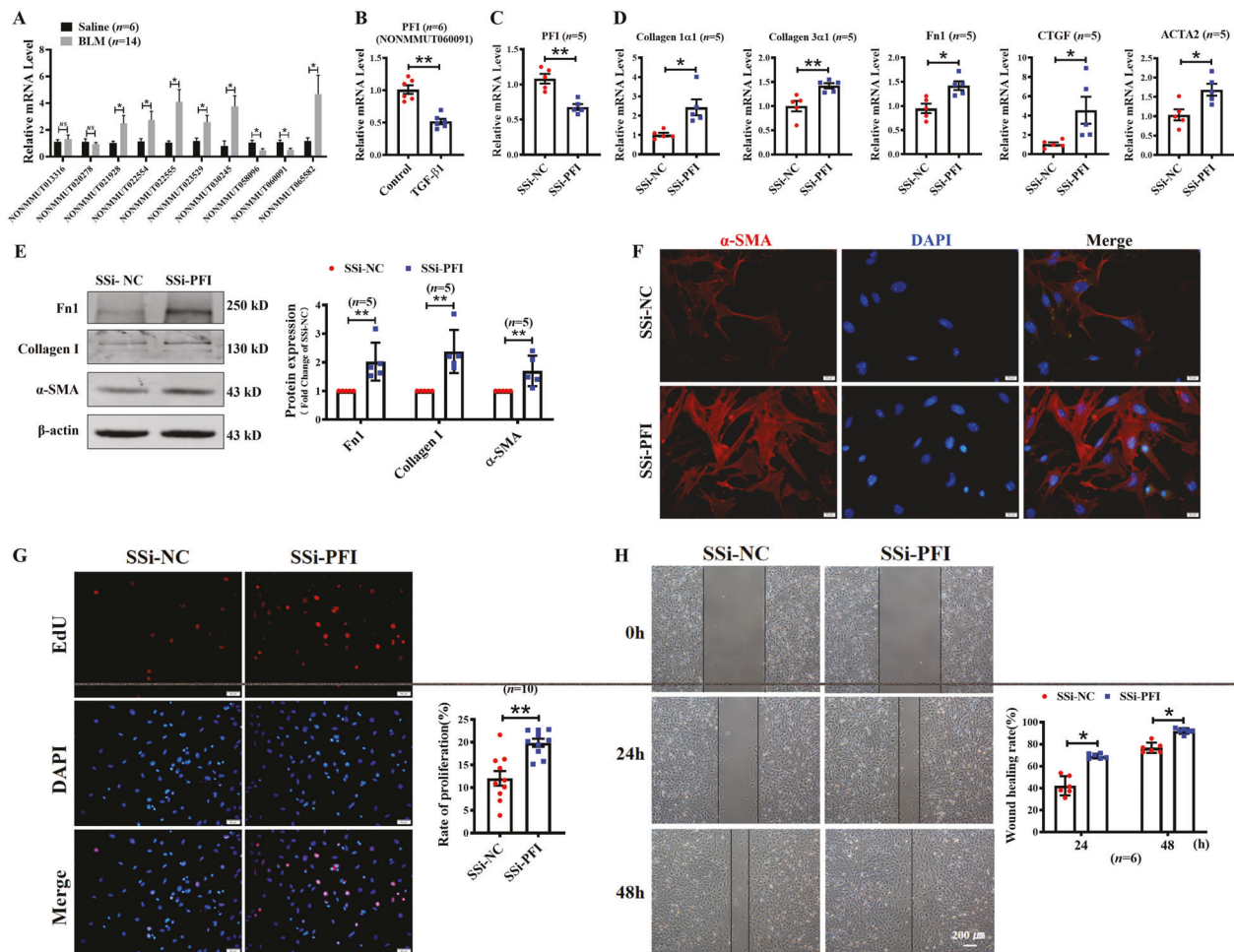


Fig. 1 Knockdown of lncRNA PFI results in fibrogenesis of MLFs. **A** qRT-PCR analysis showed six upregulated and two downregulated lncRNAs in BLM-treated mice compared to saline-treated mice. **B** lncRNA NONMMUT060091, which we named lncRNA pulmonary fibrosis inhibitor (lncRNA PFI), was dramatically reduced in TGF- β 1-treated mouse lung fibroblasts (MLFs). **C**, **D** qRT-PCR assays of relative lncRNA PFI, collagen 1 α 1, collagen 3 α 1, Fn1, CTGF, and ACTA2 expression in MLFs treated with SSi-PFI or SSi-NC. **E** Western blots demonstrated markedly increased expression of fibrosis-related proteins

Fn1, Collagen I, and α -SMA in SSi-PFI transfected MLFs. **F** Immunofluorescence staining of α -SMA suggested acceleration of the fibroblast-myofibroblast transition after silencing of lncRNA PFI; bar = 20 μ m; $n = 5$ independent experiments. **G** EdU fluorescent staining indicated that lncRNA PFI inhibition promoted the proliferation of MLFs; bar = 50 μ m. **H** A wound healing assay showed that the suppression of lncRNA PFI facilitated MLFs migration; bar = 200 μ m. * $P < 0.05$; ** $P < 0.01$. MLFs mouse lung fibroblasts, SSi-PFI PFI smart silencer, SSi-NC negative control smart silencer.

expression of collagen 1 α 1, collagen 3 α 1, Fn1, CTGF, and ACTA2 in MLF cells, which was nearly completely suppressed by PFI overexpression (Fig. 2B). In addition, Western blot assays also showed that PFI could inhibit the increase of Fn1, Collagen I, and α -SMA protein expression induced by TGF- β 1 (Fig. 2C). Through immunofluorescence experiments, we found that PFI overexpression could significantly reduce the expression of α -SMA induced by TGF- β 1, and blunt the differentiation into myofibroblasts (Fig. 2D). Through the EdU assay, we found that overexpression of PFI could significantly inhibit the proliferation of fibroblasts driven by TGF- β 1 (Fig. 2E). At the same time, as shown in Fig. 2F, forced expression of PFI significantly attenuated cell migration and abated wound healing.

Enhanced expression of lncRNA PFI prevents experimental lung fibrosis in mice

In order to evaluate the role of PFI in vivo, we constructed transgenic mice with systemic overexpression of PFI (TG-PFI) and verified the overexpression efficiency (Fig. 3A). qRT-PCR results showed that the mRNA expression levels of collagen 1 α 1, collagen 3 α 1, Fn1, and ACTA2 were up-regulated in the lungs of wild type (WT) mice after intratracheal injection of BLM, whereas none of these fibrosis-related factors showed change in BLM-treated TG-PFI mice (Fig. 3B). As shown in Fig. 3C, Western blots also showed that PFI could inhibit the increase of Fn1, Collagen I, and α -SMA at the protein level induced by BLM in the lungs. Moreover, micro-computed tomography

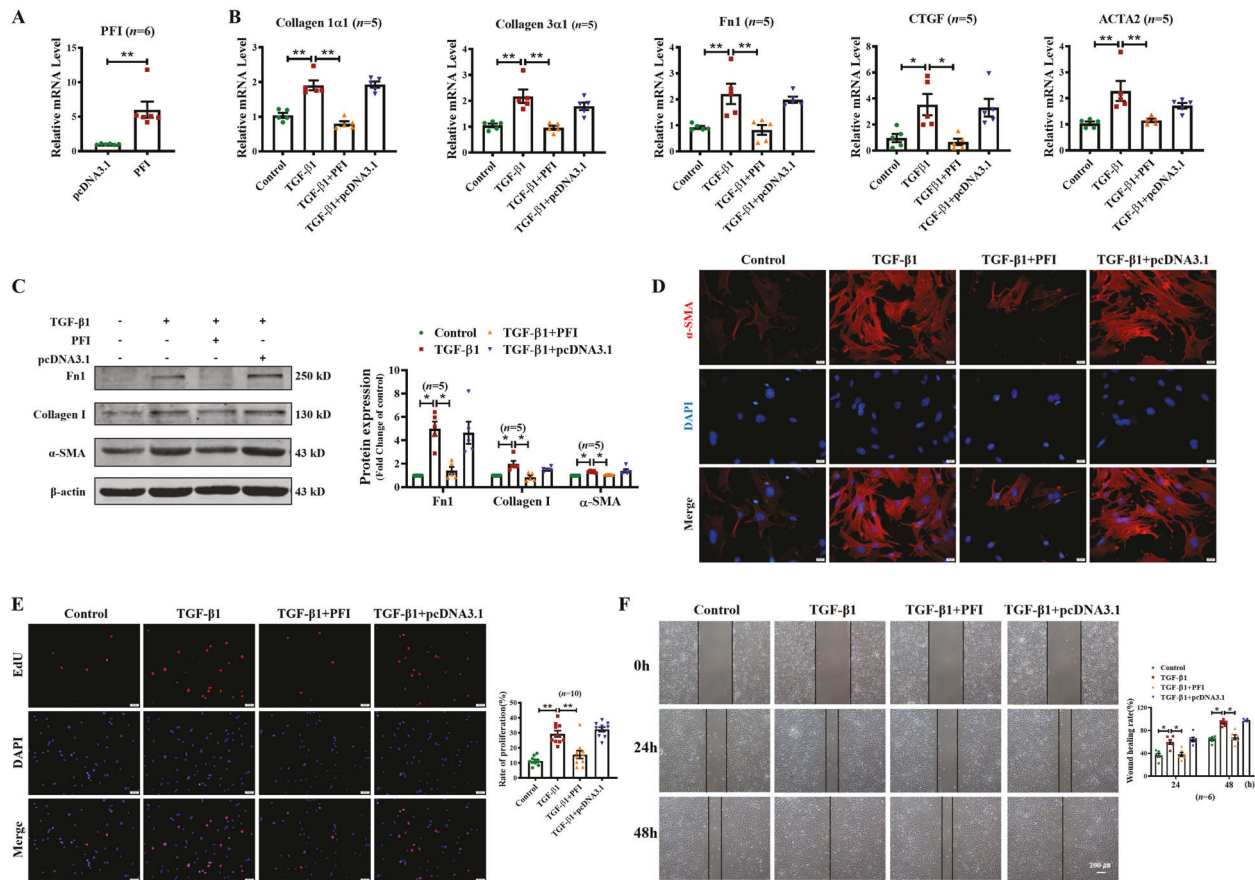


Fig. 2 Overexpression of lncRNA PFI alleviates TGF- β 1-induced fibrogenesis in MLFs. **A** Overexpression of lncRNA PFI was confirmed by qRT-PCR. **B** qRT-PCR analysis of the relative mRNA expression of collagen 1 α 1, collagen 3 α 1, Fn1, CTGF, and ACTA2 in TGF- β 1-induced MLFs transfected with lncRNA PFI. **C** Western blots showed that overexpression of lncRNA PFI abated the increased synthesis of fibrotic proteins induced by TGF- β 1. **D** Forced expression

of lncRNA PFI impeded the fibroblast-myofibroblast transition driven by TGF- β 1, as assessed by immunofluorescence assay; bar = 20 μ m; n = 5 independent experiments. **E** EdU assay (bar = 50 μ m) and **F** wound healing experiments (bar = 200 μ m) indicated that the transfection of lncRNA PFI hindered proliferation and migration of TGF- β 1-treated MLFs. * P < 0.05; ** P < 0.01. MLFs mouse lung fibroblasts.

(Micro-CT) results demonstrated that the lung shadow was increased in BLM-treated WT mice, and that such increase was relieved in BLM-treated TG-PFI mice (Fig. 3D). Moreover, H&E staining showed that the alveolar septum was destroyed and broadened in BLM-treated WT mice, whereas such effect was not present in TG-PFI mice (Fig. 3E). Meanwhile, the results of Masson staining and Collagen I immunohistochemical staining revealed that overexpression of PFI could reduce collagen deposition in the lungs of BLM-treated mice (Fig. 3E). And, the results of α -SMA immunohistochemical staining showed that overexpression of PFI could reduce the transdifferentiation of MLFs into myofibroblasts induced by BLM (Fig. 3E). In addition, the Ashcroft Score and the hydroxyproline content revealed that PFI significantly mitigated the degree of lung fibrosis and reduced collagen deposition (Fig. 3F–G). These results suggested that, consistent with the *in vitro*

experiments, forced expression of PFI alleviated BLM-induced PF in mice by reducing ECM deposition and fibroblast differentiation.

lncRNA PFI is able to bind to and regulate the expression of SRSF1

It is currently believed that how lncRNAs perform their biological function is closely related to their cellular localization [25]. Through FISH experiments, we found that lncRNA PFI mainly resides in the nucleus of MLFs (Fig. 4A). It has been found that the primary mechanism by which lncRNAs participate in the regulation of biological processes in the nucleus depends on their binding to proteins and thus regulating their expression and activity. Therefore, we performed a chromatin isolation by RNA purification-mass spectrometry (ChIRP-MS) assay to explore the proteins bound by PFI and mediating its anti-

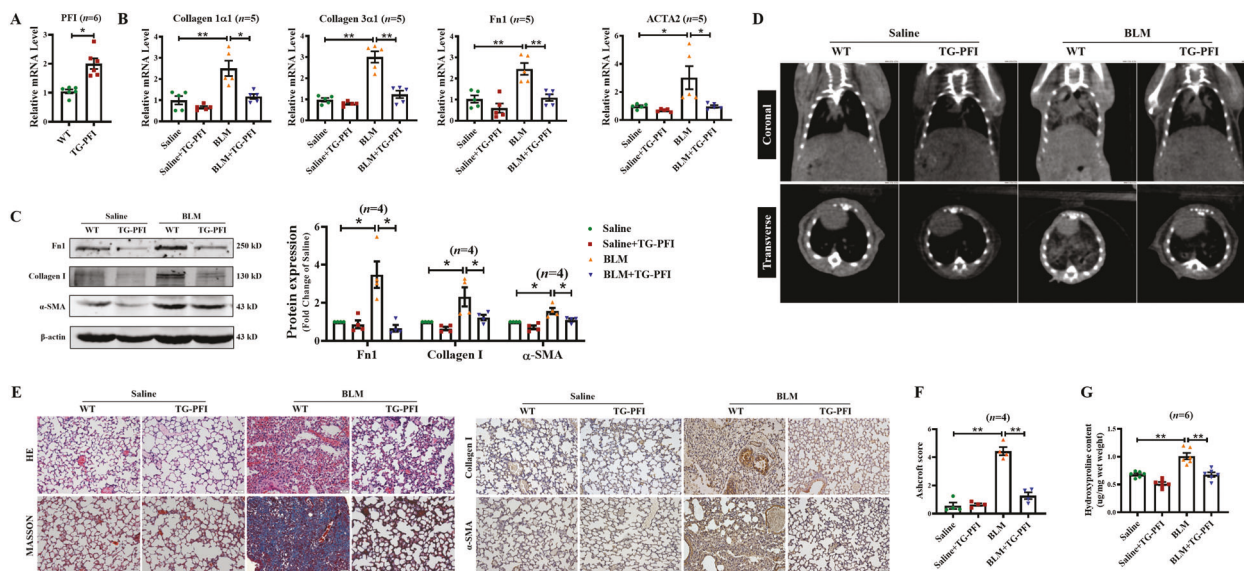


Fig. 3 Forced expression of lncRNA PFI inhibits lung fibrosis in BLM-treated mice. **A** qRT-PCR analysis of the relative expression of lncRNA PFI in WT and TG-PFI mice. **B** The mRNA expression level of collagen 1α1, collagen 3α1, Fn1, and ACTA2 decreased dramatically in BLM-treated TG-PFI mice compared with BLM-treated WT mice. **C** Western blots showed reduced fibrosis-associated protein expression in BLM-treated TG-PFI mice compared with BLM-treated WT mice. **D** Micro-CT indicated a reduced shaded area in the lungs of TG-PFI mice when exposed to BLM; *n* = 3 mice. **E** TG-PFI mice exhibited attenuated collagen deposition and more complete structure

of the alveoli as by H&E and Masson staining; Immunohistochemistry analysis showed decreased protein expression of Collagen I and α-SMA in BLM-treated TG-PFI mice compared BLM-treated WT mice; bar = 50 μm. **F** The degree of interstitial lung fibrosis were determined by using a predetermined numerical scale of 0–8, based on the Ashcroft scoring method. **G** Quantitative examination of hydroxyproline levels in lung tissue. **P* < 0.05; ***P* < 0.01. WT wild-type, TG-PFI transgenic mice of PFI, BLM bleomycin, Micro-CT micro-computed tomography.

fibrotic effects (Fig. 4B). The functional annotations of the interacting proteins were obtained from the Gene Ontology (GO) database, and pathway enrichment analysis was carried out using the Kyoto Encyclopedia of Genes and Genomes (KEGG) database. The results of these analyses showed that the interacting proteome of PFI was significantly enriched in protein complexes related to alternative splicing (Fig. 4C, D). The protein–protein interaction of some PFI-binding proteins was shown in Fig. 4E. In particular, the MS assay suggested the binding of splicing factor SRSF1 to PFI (Fig. 4F). In order to further confirm such binding, we designed a set of biotin-labeled specific probes to pull down the proteins directly bound to PFI. We used sodium dodecyl sulfate–polyacrylamide gel electrophoresis (SDS–PAGE) to separate the pulled protein complex, and the results showed that SRSF1 was indeed among in the pulled proteins (Fig. 4G). Furthermore, Western blot assays demonstrated that silencing PFI increased the expression of SRSF1, whereas overexpression of PFI inhibited TGF-β1-induced up-regulation of SRSF1 in MLFs (Fig. 4H, I). Consistent with these results, BLM administration promoted the expression of SRSF1 in WT mice, but not in TG-PFI mice (Fig. 4J). These results suggest a direct interaction between SRSF1 and PFI, which may be involved in the pathological process of PF.

Overexpression of SRSF1 induces fibrogenesis in MRC-5 cells by promoting EDA+Fn1 formation

We then constructed an adenovirus containing a SRSF1 overexpression plasmid (Adv-SRSF1) to further clarify the role of SRSF1 in the process of lung fibrosis (Fig. 5A). We found that overexpression of SRSF1 increased the mRNA expression of collagen 1α1, collagen 3α1, Fn1, CTGF, and ACTA2 in human lung fibroblasts MRC-5 cells (Fig. 5B). Meanwhile, forced expression of SRSF1 promoted the expression of Fn1, Collagen I, and α-SMA at the protein level in the same cells (Fig. 5C). Immunofluorescence showed that enhanced expression of SRSF1 could induce the expression of α-SMA and accelerate the differentiation of fibroblasts into myofibroblasts (Fig. 5D). Moreover, an EdU cell proliferation assay found that SRSF1 could significantly promote the proliferation of MRC-5 cells (Fig. 5E). At the same time, as shown in Fig. 5F, overexpression of SRSF1 could significantly promote cell migration and wound healing.

Next, we used the bioinformatics website MiasDB (<http://47.88.84.236/Miasdb/search.php>), an alternative splicing-related molecular interaction database [26], to predict the downstream targets of SRSF1. The results showed that SRSF1 could regulate the alternative splicing

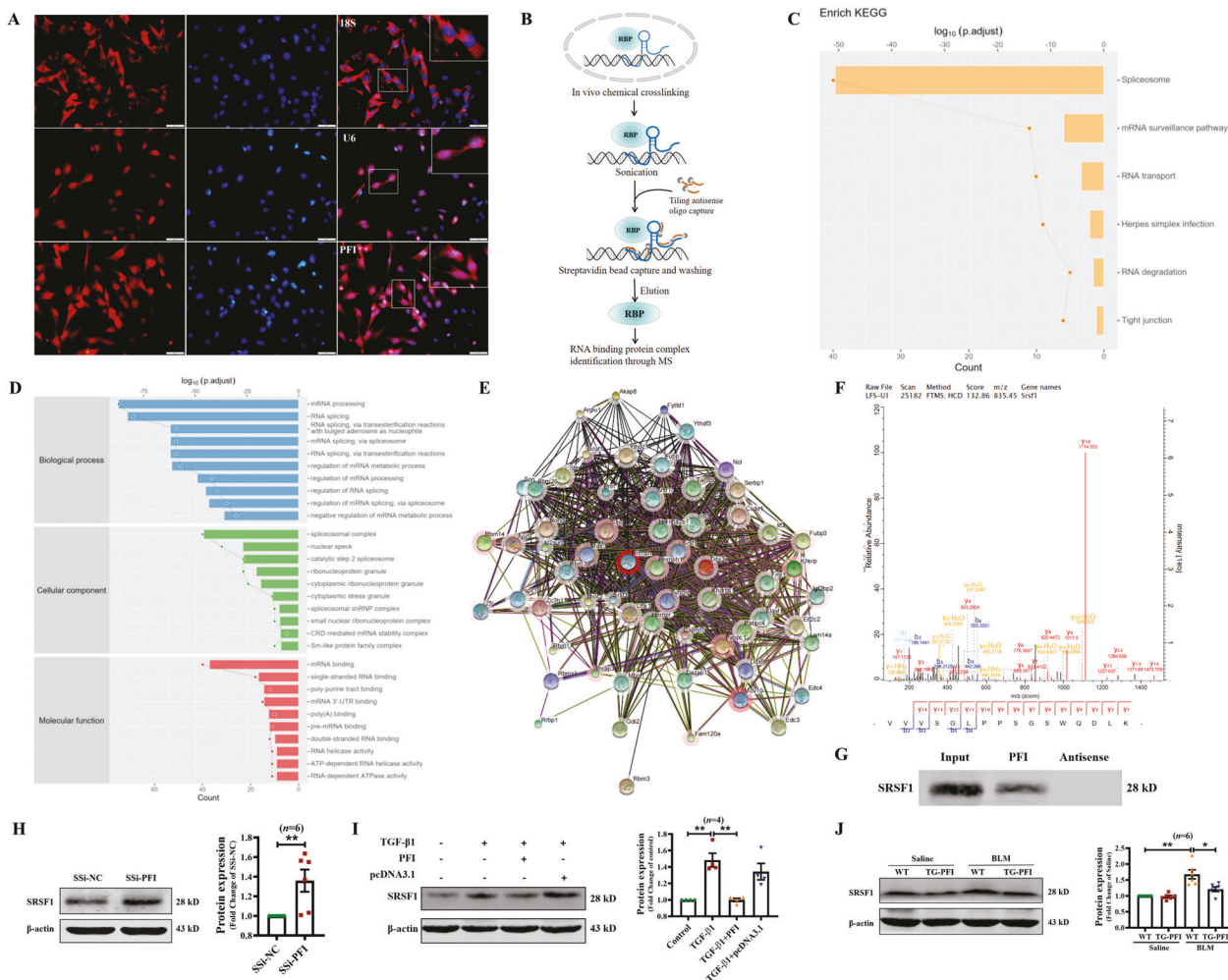


Fig. 4 LncRNA PFI is able to bind to and regulate the expression of SRSF1. **A** FISH experiment showing that lncRNA PFI was predominantly expressed in the nuclei; bar = 20 μ m. **B** Simplified schematics of ChIRP-MS. **C–E** KEGG and GO analysis of the PFI interactome demonstrated the enrichment of splicing factors among PFI-interacting proteins. **F** The protein mass spectrum suggested the binding of splicing factor SRSF1 to lncRNA PFI. **G** SDS-PAGE confirmed the binding of lncRNA PFI to SRSF1 by RNA pull-down

assay. **H** Western blot showed increased expression of SRSF1 in MLFs transfected with SSi-PFI. **I** Overexpression of lncRNA PFI abrogated the upregulation of SRSF1 protein expression induced by TGF- β 1 in MLFs. **J** Western blots indicated reduced SRSF1 expression in the lungs of TG-PFI mice exposed to BLM compared with WT mice. * $P < 0.05$; ** $P < 0.01$. ChIRP-MS chromatin isolation by RNA purification-mass spectrometry, KEGG Kyoto Encyclopedia of Genes and Genomes, GO Gene Ontology, MLFs mouse lung fibroblasts.

of the fibrosis-related gene Fn1. We then measured the expression of the EDA alternative exon: qRT-PCR and agarose gel electrophoresis showed that overexpression of SRSF1 increased the mRNA level and percent spliced in (PSI) of EDA + Fn1, an isoform of Fn1 that has more effective pro-fibrotic effects [27, 28] (Fig. 5G, H). These data show that SRSF1 promotes fibrogenesis and over-activation of MRC-5 cells by altering Fn1 splicing.

Silencing SRSF1 alleviates fibrogenesis by downregulating the EDA+Fn1 isoform

To further explore the effects of SRSF1 knockdown on fibrogenesis, we constructed three small interference RNAs

(siRNAs) against SRSF1 to silence its expression in MRC-5 cells. qRT-PCR results showed that all these three siRNAs could inhibit the expression of SRSF1 in MRC-5 cells (Fig. 6A). We then applied siRNA-2 and siRNA-3 to examine the role of SRSF1, and qRT-PCR results showed that silencing of SRSF1 inhibited TGF- β 1-induced up-regulation of collagen 1 α 1, collagen 3 α 1, Fn1, CTGF, and ACTA2 in MRC-5 cells (Fig. 6B). At the same time, the results from Western blots showed that SRSF1 inhibition alleviated TGF- β 1-driven expression of Fn1, Collagen I, and α -SMA at the protein level in the same cells (Fig. 6C). In addition, we found that silencing SRSF1 could reduce the expression of α -SMA and inhibit the differentiation of fibroblasts into myofibroblasts driven by TGF- β 1 (Fig. 6D). Moreover, an EdU cell

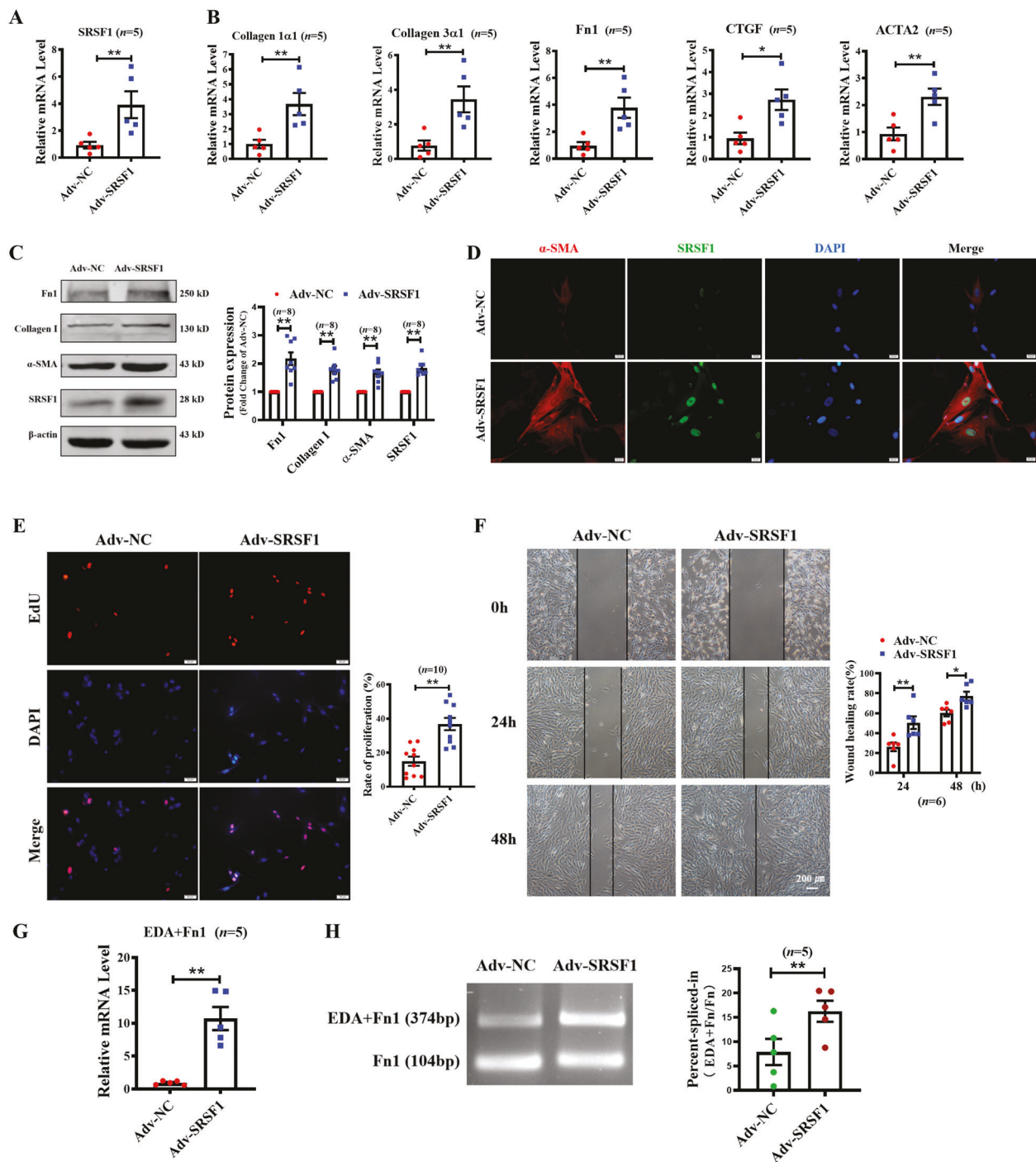
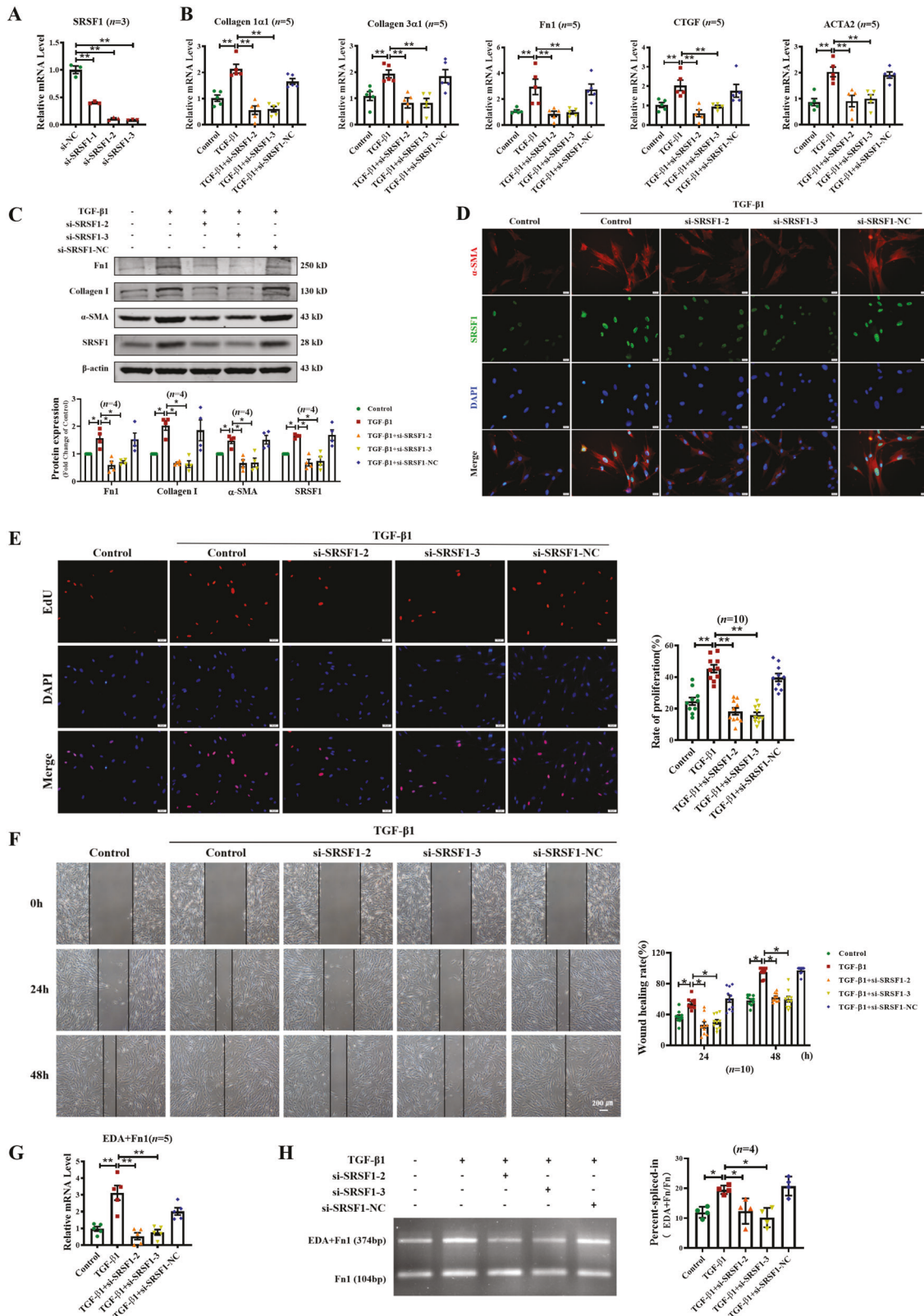


Fig. 5 Overexpression of SRSF1 induces fibrogenesis in MRC-5 cells by promoting EDA+Fn1 formation. **A** qRT-PCR analysis of relative expression of SRSF1 in MRC-5 cells treated with Adv-SRSF1. **B** qRT-PCR assay showed significantly increased mRNA expression of collagen 1 α 1, collagen 3 α 1, Fn1, CTGF, and ACTA2 in Adv-SRSF1-treated MRC-5 cells. **C** Western blots demonstrated a dramatically increased synthesis of fibrosis-related proteins after treated of Adv-SRSF1 in MRC-5 cells. **D** Fibroblast–myofibroblast transition was promoted in MRC-5 cells treated with Adv-SRSF1, as assessed by immunofluorescence; bar = 20 μ m; $n = 5$ independent experiments.

E EdU (bar = 50 μ m) and **F** wound healing assays (bar = 200 μ m) demonstrated that the forced expression of SRSF1 by Adv-SRSF1 accelerated the proliferation and migration of MRC-5 cells. **G** qRT-PCR analysis showed markedly upregulated synthesis of the EDA + Fn1 mRNA after treated of Adv-SRSF1 in MRC-5 cells. **H** The percent spliced-in (PSI) of EDA + Fn1 was significantly increased in SRSF1-overexpressing MRC-5 cells, as demonstrated by agarose gel electrophoresis. * $P < 0.05$; ** $P < 0.01$. Adv-SRSF1 SRSF1 overexpression adenovirus.



◀ **Fig. 6 Silencing SRSF1 attenuates fibrogenesis by downregulating the EDA + Fn1 isoform.** **A** qRT-PCR showed the silencing efficacy of siRNAs against SRSF1. **B** qRT-PCR analysis of the relative expression of fibrosis-related genes in TGF- β 1-induced MRC-5 cells transfected with si-SRSF1 or si-NC. **C** Western blots demonstrated that SRSF1 knockdown by siRNA abated TGF- β 1-induced up-regulation of fibrosis-associated proteins. **D** Immunofluorescence suggested that silencing SRSF1 impeded the fibroblast–myofibroblast transition in TGF- β 1-treated MRC-5 cells; bar = 20 μ m; $n = 6$ independent experiments. **E** EdU (bar = 50 μ m) and **F** wound healing (bar = 200 μ m) assays indicated that SRSF1 knockdown inhibited the proliferation and migration of MRC-5 cells. **G** qRT-PCR analysis of the relative expression of EDA + Fn1 in si-SRSF1-transfected MRC-5 cells induced by TGF- β 1. **H** Agarose gel electrophoresis showed a significantly decreased PSI of EDA + Fn1 in TGF- β 1-treated MRC-5 cells after transfection with si-SRSF1. * $P < 0.05$; ** $P < 0.01$. PSI percent spliced in.

proliferation assay showed that SRSF1 knockdown could markedly inhibit the proliferation of MRC-5 cells (Fig. 6E). At the same time, as shown in Fig. 6F, inhibition of SRSF1 could significantly attenuate TGF- β 1-induced cell migration and slow down wound healing. Furthermore, the results of qRT-PCR and agarose gel electrophoresis showed that the silencing of SRSF1 reduced the expression of the EDA + Fn1 isoform (Fig. 6G, H).

Anti-fibrotic effects of lncRNA PFI in MRC-5 cells: potential application of PFI

We then transfected PFI into MRC-5 cells to examine whether PFI plays a anti-fibrotic effect in human lung fibroblasts. As shown in Fig. 7A, we found that overexpression of PFI alleviated TGF- β 1-induced up-regulation of fibrosis-related genes, including collagen 1 α 1, collagen 3 α 1, Fn1, CTGF, and ACTA2. Consistent with these results, Western blot assays showed that PFI overexpression significantly inhibited the increase of Fn1, Collagen I, and α -SMA associated to the fibrogenesis of MRC-5 cells driven by TGF- β 1 (Fig. 7B). We also found that forced expression of PFI also ablated the up-regulation of SRSF1 in TGF- β 1-treated MRC-5 cells, consistent with the results obtained in MLFs (Fig. 7B). Furthermore, an immunofluorescence assay showed that overexpression of PFI could significantly reduce the expression of α -SMA induced by TGF- β 1, and blunted the differentiation of fibroblasts into myofibroblasts, as well as the expression of SRSF1 in the nucleus (Fig. 7C). Moreover, an EdU proliferation assay found that overexpression of PFI could significantly inhibit the proliferation of MRC-5 cells induced by TGF- β 1 (Fig. 7D). At the same time, as shown in Fig. 7E, enhanced expression of PFI significantly attenuated cell migration and ablated wound healing. More importantly, we also found that forced expression of PFI markedly inhibited the formation of the EDA + Fn1 isoform and reduced its relative contribution to the expression of Fn1 (Fig. 7F, G). These results showed that

PFI exerts its anti-fibrotic effect through regulating SRSF1 to alter Fn1 splicing also in human lung fibroblasts, indicating its potential application in lung fibrosis.

lncRNA PFI reverses established lung fibrosis in a BLM model through regulation of SRSF1

In order to further clarify the therapeutic effect of PFI in vivo and whether such effect is mediated by SRSF1, adenovirus-associated viruses 5 (AAV-5) containing PFI or an SRSF1 overexpression plasmid were established and designated as AAV5-PFI and AAV5-SRSF1, respectively. AAV5-PFI was intratracheally injected with or without AAV5-SRSF1 five days before administration of BLM, and the mice were euthanized after 3 weeks (Fig. 8A–C). qRT-PCR results showed that forced expression of lncRNA PFI had no effect on fibrosis-associated proteins in untreated mice (Fig. 8D). However, overexpression of PFI significantly alleviated the up-regulation of collagen 1 α 1, collagen 3 α 1, Fn1, and ACTA2 in BLM-treated mice, whereas enhanced expression of SRSF1 abolished the beneficial action of PFI (Fig. 8D). Moreover, Western blots showed that overexpression of PFI restored the BLM-induced upregulation of fibrosis-related proteins Fn1, Collagen I, and α -SMA, and also inhibited the expression of SRSF1 in BLM-treated mice. These regulatory changes were abated by the addition of AAV5-SRSF1 (Fig. 8E). As shown in Fig. 8F, the alveolar septum was destroyed and broadened, and this was accompanied by infiltration of inflammatory cells in the lungs of BLM-treated mice. In agreement with these results, enhanced expression of lncRNA PFI mitigated ECM deposition, collagen formation, and myofibroblast activation in BLM-treated mice, an inhibition which was effectively restored by the addition of the AAV5-SRSF1 (Fig. 8F, G). The data from hydroxyproline content assay showed that forced expression of PFI alleviated the BLM-induced hydroxyproline content in mice, whereas enhanced expression of SRSF1 abolished the beneficial action of PFI (Fig. 8H). These data show that forced expression of PFI reverses the BLM-induced lung fibrosis in mice through the regulation of SRSF1.

Discussion

In the present study, we characterized the anti-fibrotic effect of lncRNA PFI and the underlying mechanism in both BLM-induced mouse lung fibrosis and TGF- β 1-driven fibrogenesis in human lung fibroblasts. We found that silencing PFI promoted, whereas overexpression of PFI alleviated, lung fibrosis in vitro and in vivo through binding to and regulating the expression and activity of SRSF1, and thereby inhibiting fibroblast over-activation, reducing excessive ECM deposition, and attenuating

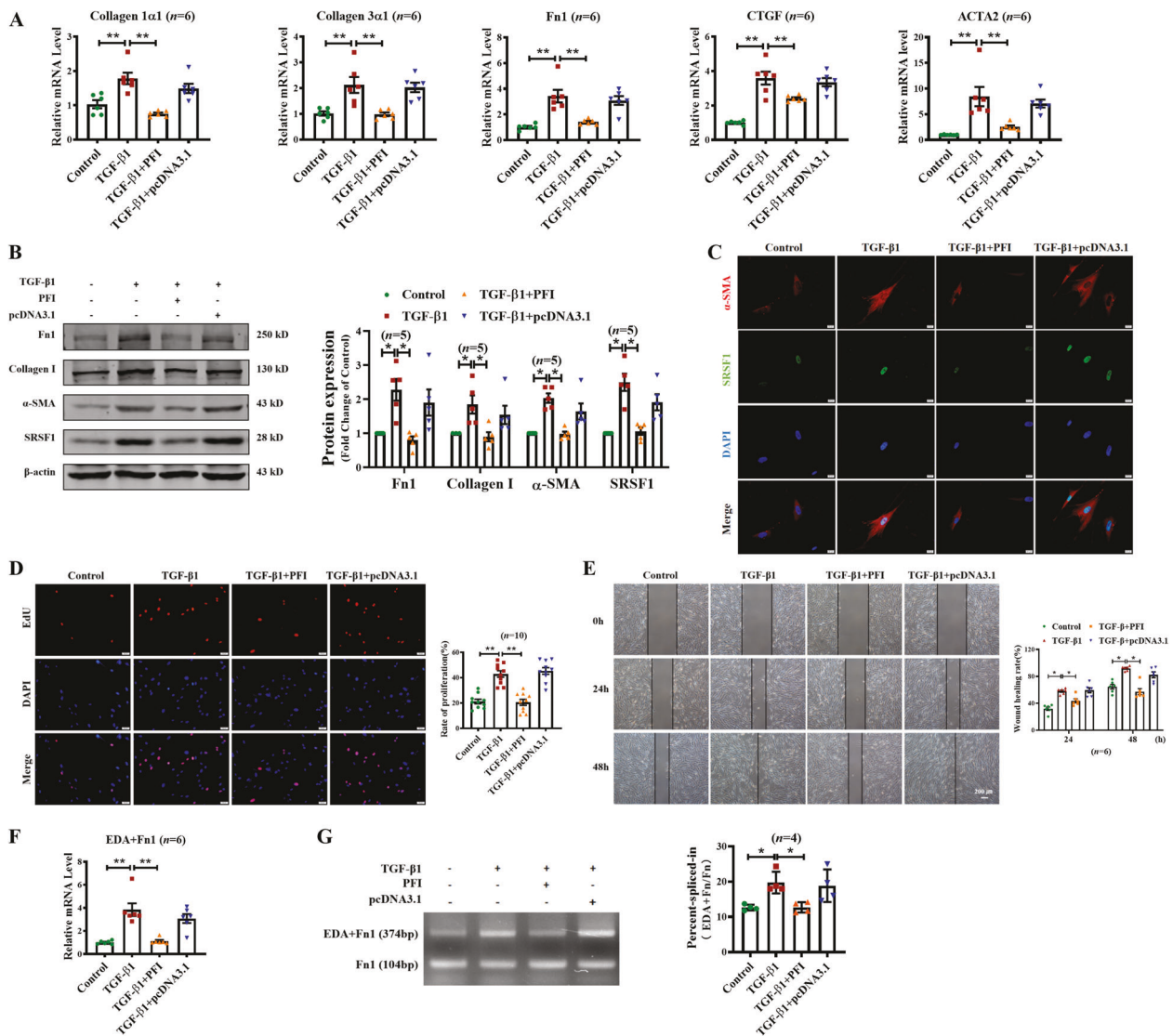


Fig. 7 Enhanced expression of PFI inhibits TGF-β1-induced fibrogenesis in MRC-5 cells. **A** qRT-PCR analysis demonstrating the relative expression of collagen 1α1, collagen 3α1, Fn1, CTGF, and ACTA2 in TGF-β1-induced MRC-5 cells transfected with or without lncRNA PFI. **B** Western blots suggested that the forced expression of lncRNA PFI abrogated the upregulation of fibrotic proteins in MRC-5 cells induced by TGF-β1. **C** Immunofluorescence indicated that overexpression of lncRNA PFI inhibited the fibroblast–myofibroblast transition in TGF-β1-treated MRC-5 cells; bar = 20 μm; n = 8

independent experiments. **D** EdU (bar = 50 μm) and **E** wound healing (bar = 200 μm) assays showed that the transfection with lncRNA PFI blocked the proliferation and migration of MRC-5 cells in the presence of TGF-β1. **F** The relative expression of EDA + Fn1 was dramatically reduced in lncRNA PFI-overexpressing MRC-5 cells as determined by qRT-PCR. **G** Agarose gel electrophoresis suggested significantly decreased PSI of EDA + Fn1 in TGF-β1-treated MRC-5 cells after transfected with lncRNA PFI. **P* < 0.05; ***P* < 0.01. PSI percent spliced in.

the fibroblast–myofibroblast transition. Furthermore, we found that overexpression of SRSF1 resulted in lung fibroblasts activation by promoting the formation of the EDA + Fn1 splicing isoform (Fig. 8I). In contrast, SRSF1 knockdown inhibited fibrogenesis in MRC-5 cells. Moreover, enhanced expression of SRSF1 abrogated the anti-fibrotic action of PFI in BLM-treated mice. More importantly, this study showed that forced expression of PFI alleviated TGF-β1-induced fibrogenesis in MRC-5 cells. These results suggest that PFI replacement

or targeting of SRSF1 might be considered promising strategies for the treatment of lung fibrosis.

More and more studies, including ours, have demonstrated that lncRNAs participate in the process of lung fibrosis. In previous studies, we found that both PFAL and PRFL promote the occurrence and development of fibrosis through the mechanism of ceRNA. Among them, lncRNA PFAL participates in regulating the expression level of downstream effector molecule CTGF and then affects the

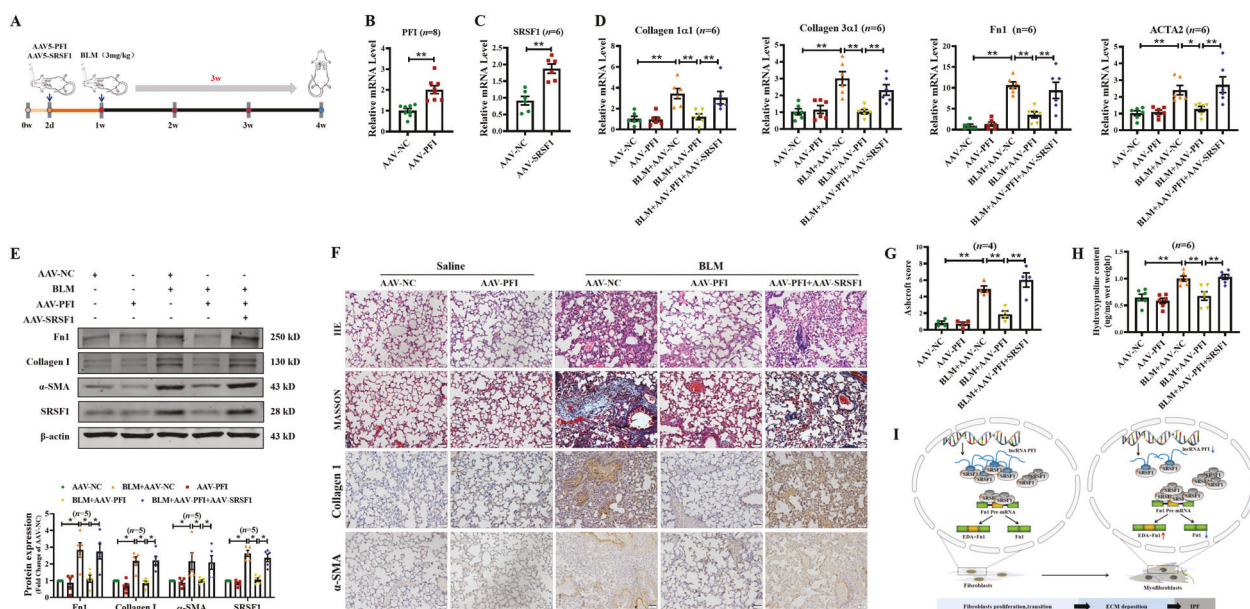


Fig. 8 SRSF1 is necessary for the anti-fibrotic effects of lncRNA PFI in a bleomycin model. **A** Schematic diagram of the experimental design. Mice were intratracheally injected with AAV5-PFI and AAV5-SRSF1 five days ahead of bleomycin (BLM) treatment. Lungs were harvested after 3 weeks. **B**, **C** qRT-PCR analysis of the relative expression of lncRNA PFI and SRSF1 after the injection of AAV5-PFI and AAV5-SRSF1. **D** qRT-PCR analysis of the relative expression of collagen 1 α 1, collagen 3 α 1, Fn1, and ACTA2 in the lungs of BLM-treated mice injected with AAV5-PFI, AAV5-SRSF1, or both. **E** Western blots indicated that lncRNA PFI inhibited the upregulation of fibrosis-related protein expression induced by BLM. **F** H&E and Masson staining showed that the overexpression of lncRNA PFI reduced inflammatory infiltrates and abrogated excessive ECM deposition in BLM-treated mice lungs. Immunohistochemistry analysis suggested

reduced synthesis of Collagen I and α -SMA in the lungs injected with lncRNA PFI, which was abrogated by overexpression of SRSF1; bar = 50 μ m; $n = 4$ mice. **G** Morphological changes in lungs were quantified by the Ashcroft score. **H** Hydroxyproline content of lung tissues in different groups. **I** Proposed model for the mechanism by which lncRNA PFI binds to SRSF1 to inhibit its function on alternative splicing. The biosynthesis of EDA + Fn1 is limited, which maintains the quiescent state of fibroblasts. After stimuli, the decreased expression of PFI results in activation of SRSF1 which leads to abundant expression of EDA + Fn1, thus promoting the proliferation of lung fibroblasts and their transition to myofibroblasts, along with the excessive deposition of ECM ultimately causing pulmonary fibrosis. * $P < 0.05$; ** $P < 0.01$. AAV5-PFI (AAV5-SRSF1) adenovirus-associated viruses 5 containing PFI (SRSF1) overexpression plasmid.

process of PF through competitive binding with miR-18a [29], in addition, lncRNA PFRL can promote fibrogenesis and mouse lung fibrosis through targeted intervention of miR-26a/p-Smad3 loop [30]. These results have contributed to the clarification of the mechanism of competing endogenous RNAs (ceRNAs). In this study, we found that PFI may play an important role in the pathogenesis of lung fibrosis by binding the SRSF1 protein, providing further insight in the role of lncRNAs in the PF regulatory network.

Although many studies have confirmed the role of lncRNAs in organ fibrosis, including lung fibrosis, the application of their results is often limited due to the low homology and conservation of lncRNAs. Recently, Translate Bio (formerly RaNA Therapeutics) and OPKO Health used diverse methods to selectively up-regulate individual genes by blocking their regulatory lncRNAs with oligonucleotide-based drugs [31, 32]. Advances in the understanding of the mechanism of action of lncRNAs will contribute to the development of lncRNA-targeted treatments. A promising area of research is the targeting of several lncRNAs

simultaneously. Multimers and multi-targeting oligonucleotides could be designed to increase the in vivo efficacy against single or multiple lncRNA targets [33]. In this study, we screened the differentially expressed lncRNAs in fibrosis in order to find those that could interfere with its progression. Among these, importantly, PFI not only plays an anti-fibrotic effect in mice, but also reduces fibrogenesis in human lung fibroblasts. Therefore, it holds tremendous potential to be used in human lung fibrosis. Our results provide a theoretical basis for the development of lncRNA-targeting drugs and, more generally, of therapeutic methods based on the targeting of non-coding RNAs in PF.

The mechanism and action of lncRNAs depends on their cellular localization. Through FISH assays, PFI is found in both the cytoplasm and the nucleus of MLFs. We systematically assessed the interactome map of PFI through a ChIRP-MS high-throughput identification technique. GO and KEGG analysis of the results suggest that PFI is closely related to the alternative splicing of RNA, its interacting proteins mainly including the HNRNP, SR, and RBM

protein families, and others. Among these, we focused on the splicing factor SRSF1, which showed high binding coefficient among the binding proteins, and further verified the binding of PFI to the SRSF1 protein by RNA pull-down. More importantly, we found that SRSF1 was necessary for and mediated the anti-fibrotic effects of PFI in lung fibrosis.

SRSF1 was originally discovered as a splicing factor. An increasing number of studies have shown that SRSF1 is up-regulated in many tumors, such as breast tumors, lung tumors, colon tumors, kidney tumors, and acute lymphoblastic leukemia [34]. In view of the fact that SRSF1 regulates the alternative splicing of oncogenes and tumor suppressor genes, and participates in the occurrence and development of tumors, it might be a possible tool for tumor diagnosis, and a potential therapeutic target in a broad variety of tumors. However, the function of SRSF1 in fibrosis is not clear yet. Previous work has shown that SRSF1, as an oncogene, promotes tumor progression by promoting gene splicing alterations [35, 36]. Besides, it has been reported that SRSF1 increases proliferation and delays apoptosis of breast epithelial cells and promotes cell transformation [37]. In the current study, we found for the first time that SRSF1 plays a vital role in promoting the fibrogenesis of lung fibroblasts during PF. Cramer et al. reported that SRSF1 and 9G8 stimulate EDA + Fn1 alternative splicing in vivo [38]. High expression of SRSF1 in the endometrium also promotes EDA + Fn1 expression, and plays a central role not only in tumor cells, but also in the surrounding stroma [39]. However, EDA + Fn1 is less expressed in normal tissues and has a more substantial effect on promoting cell cycle, ECM deposition, and cell differentiation than Fn1. We found that SRSF1 promotes the production of the EDA + Fn1 isoform in PF, thus promoting cell proliferation, differentiation, and collagen deposition. Our study revealed, for the first time, the role of SRSF1 in PF, suggesting more generally that splicing factors may play a crucial role not only in tumors but also in fibrotic diseases.

However, the current study has certain limitations. We did not identify the specific fragments of PFI that bind SRSF1, limiting our in-depth exploration of the relationship between PFI and SRSF1. In addition, the BLM-induced mouse model of lung fibrosis we used does not directly reflect human diseases resulting in fibrogenesis in the lung, so that further studies will be needed to see whether PFI can be therapeutically targeted in humans.

Taken together, the results of present work demonstrated that lncRNA PFI participates in the regulation of lung fibrosis by inhibiting the EDA + Fn1 splicing isoform production through binding to and inhibiting the expression and activity of SRSF1. Therefore it is possible to conjecture that induced expression of PFI may provide a novel approach for the prevention and treatment of PF.

Materials and methods

Mouse model of pulmonary fibrosis

Male C57BL/6 mice were raised under controlled temperature (25 °C) and humidity conditions (45% RH), with a 12-h light/dark cycle. Mice aged 6–8 weeks with an average body weight of 20–22 g were anesthetized by intraperitoneal injection of Avertin (250 mg/kg), and the mice were intratracheally injected with BLM (3 mg/kg) or saline. PF model formed 21 days later, and all mice were euthanized. Lung tissues were collected and immediately frozen in liquid nitrogen or fixed with 4% paraformaldehyde for further study. Animals were randomly assigned for each experimental group. Assessors were un-blinded to group allocation. The sample sizes is ≥ 3 for each condition. No statistical methods were used to pre-determine sample sizes.

PFI transgenic (TG-PFI) mice

Systemic overexpressed transgenic mice with PFI were constructed by Cyagen Biosciences Inc. (Guangzhou, China). PFI gene was injected into 0.5-day-old FVB/N fertilized eggs by microinjection, and then the fertilized eggs were implanted into the oviducts of female mice to develop into transgenic animals carrying exogenous PFI. The young mice were identified by PCR.

Cell culture and treatment

The human lung fibroblasts (MRC-5) was placed in MEM medium containing 10% fetal bovine serum (FBS), containing Gluta-max dipeptide 1 ml, non-essential amino acid (NEAA) 1 ml, sodium pyruvate solution 1 ml, 100 U/ml penicillin Gray 100 U/ml streptomycin, cultured in a 5% CO₂ incubator at 37 °C. MRC-5 authentication was confirmed by short tandem repeat (STR) profiling and free from mycoplasma contamination. Primary lung fibroblasts were isolated and cultured from the lungs of 3-day-old KM mice. Under aseptic condition, the lung lobe was placed in a Petri dish containing DMEM, blood vessels and other tissues were cut and chopped, and digested by 0.5 mg/ml trypsin. The cells were precipitated by centrifugation and cultured in complete medium (90% DMEM medium + 10% FBS). After 6 h, the non-adherent cells were removed by differential speed. TGF- β 1 (Sigma-Aldrich, USA) was used at a final concentration of 10 ng/ml. The cells were cultured in the medium containing TGF- β 1 for 24 h before being collected for further analysis.

Histological and immunohistochemical staining

The fresh lung tissue was fixed with 4% paraformaldehyde for 1 day, transferred to different concentrations of ethanol, dehydrated and embedded in paraffin, and the sections were stained with H&E and Masson. The tissue sections were incubated in citrate buffer (pH = 6.0) for 5 min for antigen repair, pretreated at room temperature at 3% H₂O₂ for 15 min, and then washed with PBS. Then the goat serum was incubated for 20 min. Incubate an anti-moisture box at 4 °C overnight. The second antibody (horseradish peroxidase-conjugated anti-rabbit IgG), was incubated the next day and stained with diaminobenzidine (DAB). The Ashcroft score was used to analyze the degree of PF by evaluating the images from five random fields of H&E staining for each mouse.

Immunofluorescence staining

The cultured MRC-5 cells or primary mice lung fibroblasts were placed and cultured in a six-well plate, and the treatment was given when the cell density reached 30%. Cells were washed with PBS for three times and fixed in 500 µl 4% paraformaldehyde, 37 °C, 15 min. Then incubated at room temperature for 1 h with 500 µl penetrating solution (1 ml PBS + 4 µl Triton+0.01 g BSA); blocked for 1 h with 1 ml 50% goat serum (goat serum: PBS = 1:1); Primary antibody α-SMA (ab7817, Abcam, 1:200; and SRSF1 (12929-2-AP, Proteintech, 1:50) incubations were performed overnight at 4 °C and incubation with secondary antibody for 1 h; The nucleus were stained with DAPI for 5 min at room temperature. The cells were observed under fluorescence microscope.

Real-time quantitative PCR (qRT-PCR)

The total RNA of tissue or cell samples was extracted by TRIzol reagent. The concentration and purity of the extracted RNA were determined by NanoDrop 8000 (Thermo, USA) and reverse transcribed to cDNA. All cDNA samples were prepared into 20 µl reaction system. Reaction conditions: 95 °C, 5 min; 95 °C, 10 s; 55 °C, 15 s; 72 °C, 20 s. The data were analyzed by 2^{-ΔΔCT} method. The Fn1 PCR products were analyzed by agarose gel electrophoresis, and the PCR products were verified to be in line with the predicted size.

Western blot

The total protein was extracted from the tissue or cells with RIPA lysis buffer. The quality standardized sample was mixed with 6× buffer and heated to 100 °C for 7 min. 10% SDS–polyacrylamide gel was configured. After electrophoresis, the proteins were transferred to a nitrocellulose membrane. The antibody against Fn1 (15613-1-AP, Proteintech, 1:500),

Collagen I (WL0088, Wanleibio, 1:500), SRSF1 (12929-2-AP, Proteintech, 1:300), α-SMA (AF1032, Affinity, 1:1000), and β-actin (20536-1-AP, Proteintech, 1:1000) was incubated at 4 °C overnight. The protein bands were developed and analyzed by Odyssey infrared imaging system.

ChIRP-MS

The interaction complexes of intracellular RNA with protein and nucleic acid were immobilized by formaldehyde cross-linking, and then the protein and nucleic acid complexes binding to RNA were purified by biotin-labeled probe and streptavidin magnetic beads. The proteins in the separated products were identified by mass spectrometry, and the proteins that bind to the target RNA can be screened. For each specific lncRNA molecular sequence, a specific antisense oligonucleotide sequence with a length of 20 bases was designed according to the step size of 100 nt, and all sequences were numbered. The lncRNA ChIRP probe of terminal modified Biotin-TEG group was synthesized by odd number group and even number group. LncRNA ChIRP probe was hybridized specifically with the cross-linked lncRNA molecular complex, and the Biotin-TEG chemical group was modified at the end, and the chromatin complex bound to the target lncRNA was purified by using streptavidin-coupled magnetic beads. The purified protein from the complex was digested into a mixture of peptides by protease, and then analyzed by mass spectrometer. The first and second mass spectrometric peak maps were output for protein identification.

EdU cell proliferation assay

EdU cell proliferation kit (RiboBio, Guangzhou, China) was used to detect cell proliferation by EdU (5-ethynyl-20-deoxyuridine) assay. MLFs/MRC-5 cells (1 × 10⁵/well) were inoculated into each well of 24-well plate. After treatment, the cells were incubated at 37 °C and 5% CO₂ for 48 h, then 200 µl 50 µM EdU was added to the cells and incubated for another 2 h. The cells were then fixed with 4% paraformaldehyde and stained with Apollo Dye Solution to proliferate cells. The nucleus was stained with DAPI. The cell proliferation rate was calculated according to the manufacturer's instructions. Fluorescence microscope was used to take images.

Wound healing assay

To test the cell migration ability of MLFs/MRC-5, the in vitro wound healing assay was performed. Cells were seeded in six-well plates until the cells formed a confluent monolayer, then scratched using a 100 µL pipette tip. The scratch wounds were captured using phase-contrast

microscopy at 0, 24, 48 h. The relative wound size at each time point was analyzed by Image J.

Fluorescence in situ hybridization (FISH)

In order to identify the expression location of PFI, lncRNA was labeled with probe. The slide was fixed in the newly prepared 4% paraformaldehyde aqueous solution for 10 min and washed for three times in 1× PBS for 5 min. After penetrating with 0.4% Triton-X100 for 10 min and blocking with 1% BSA, the cells were hybridized in 200 µl pre-hybridization buffer (1% blocking solution, 99% pre-hybridization) at 37 °C for 30 min. The 2.5 µl 20 µM lncRNA FISH probe mixture or internal control FISH probe mixture was then added to each well (1% closed solution, 99% pre-hybridization) overnight at 37 °C. The nucleus was restained with DAPI. Fluorescence microscope was used to take images.

Micro-CT of mouse lung

On the 21st day after the establishment of BLM model, the lung tissue density of mice was quantitatively measured by CT, and the degree of PF in each group was evaluated. CT plain scan was performed by the following methods: after anesthesia, the mice were placed on the scanning bed and kept in a supine position, then the chest of the mice was fixed with tape, and the living lung tissue of the mice was scanned after setting the scanning parameters. The scanning parameters were as follows: 120 kV, 100 mA, 0.5 mm slice was used, and the distance between slices was 0.5 mm, to cover the whole mouse chest (the total collection time was 0.5 s). The images were automatically generated by the system workstation, and then the images were post-processed by the relevant software of the system. According to the obtained images, the structural and morphological changes of lung tissue were observed to evaluate the difference of the degree of PF in mice.

RNA-pull down

First, RNA was pretreated to form a secondary structure, and then total cellular proteins were extracted. The total protein was first preincubated with 60 µl streptavidin coated with lytic solution, and the lipopolysaccharide column (Streptavidin beads), was rotated slowly at room temperature for 1 h to eliminate the background of binding to beads in the total protein. RNA was incubated with cell lysate for 1 h and then incubated with beads coated with streptavidin. After washing the beads, add 1× protein sample buffer 30 µl to the washed beads, mix them repeatedly, and heat them in boiling water for 10 min. After the sample passed western blot at 10% SDS-PAGE electrophoresis, the SRSF1 target band was detected.

Hydroxyproline assay

Hydroxyproline concentrations in lung tissues were measured with a hydroxyproline assay kit (Cat No. A030-2-1, Nanjing Jiancheng Bio Co., Nanjing, China). 40 mg wet heavy lung tissue was accurately weighed, and then experiment steps were performed following the kit instructions. The absorbance of each sample was then measured at 550 nm.

Statistical analysis

All the statistical tests were justified as appropriate. The experimental data all conform to the normal distribution. No estimate of variation has been performed within each group of data prior to statistical analysis. Variance is similar between comparison groups. Data were presented as the mean ± SEM of at least three independent experiments. Significances were calculated using two-tailed *t*-test or one-way analysis of variances (ANOVA) with post-test Bonferroni-corrected *t*-test as post hoc test. $P < 0.05$ was considered statistically significant difference. Statistical analyses were carried out using GraphPad Prism 8.0.

Data availability

The ChIRP-MS data has been uploaded as Supplementary Table 1. All data that support the findings of this study are available from the corresponding author upon reasonable request.

Acknowledgements We thank Prof. Yanjie Lu very much for providing the transgenic mice and plasmid of PFI, and the early contributions to the project.

Author contributions H-HL and H-LS conceived the project, designed the experiments and edited the manuscript. JS, X-LL, Y-HZ planned the experiments, integrated data and wrote the manuscript. JS, T-ZJ, WS, Y-YG, J-YW performed cellular and molecular biological experiments, executed data analysis. Z-HN, J-YG, TY, L-LL, LM performed animal studies and analyzed the data.

Funding This study was supported by the National Natural Science Foundation of China (91949109, 81770284, 31671187, 81870211, 81872863); the Major Scientific Fund Project of Heilongjiang Province (ZD2019H001); and the the CAMS Innovation Fund for Medical Sciences (CIFMS, 2019-I2M-5-078).

Compliance with ethical standards

Conflict of interest The authors declare no competing interests.

Ethics statement All animal experiments were approved by the Harbin Medical University Animal Ethical committee (No. IRB300720) and conformed to the Declaration of Helsinki.

Publisher's note Springer Nature remains neutral with regard to jurisdictional claims in published maps and institutional affiliations.

References

1. Maher TM, Wuyts W. Management of fibrosing interstitial lung diseases. *Adv Ther.* 2019;36:1518–31.
2. Richeldi L, Collard HR, Jones MG. Idiopathic pulmonary fibrosis. *Lancet.* 2017;389:1941–52.
3. Taskar V, Coultas D. Exposures and idiopathic lung disease. *Semin respir Crit Care Med.* 2008;29:670–9.
4. Chioma OS, Drake WP. Role of microbial agents in pulmonary fibrosis. *Yale J Biol Med.* 2017;90:219–27.
5. Molyneux PL, Maher TM. The role of infection in the pathogenesis of idiopathic pulmonary fibrosis. *Eur Respir Rev* 2013;22:376–81.
6. Tian Y, Li H, Qiu T, Dai J, Zhang Y, Chen J, et al. Loss of PTEN induces lung fibrosis via alveolar epithelial cell senescence depending on NF- κ B activation. *Aging Cell.* 2019;18:e12858.
7. Yang IV, Schwartz DA. Epigenetics of idiopathic pulmonary fibrosis. *Transl Res.* 2015;165:48–60.
8. Sack C, Raghu G. Idiopathic pulmonary fibrosis: unmasking cryptogenic environmental factors. *Eur Respir J.* 2019;53:2.
9. Meyer KC. Pulmonary fibrosis, part I: epidemiology, pathogenesis, and diagnosis. *Expert Rev Respir Med.* 2017;11:343–59.
10. Noble PW, Barkauskas CE, Jiang D. Pulmonary fibrosis: patterns and perpetrators. *J Clin Investig.* 2012;122:2756–62.
11. Taniguchi H, Ebina M, Kondoh Y, Ogura T, Azuma A, Suga M, et al. Pirfenidone in idiopathic pulmonary fibrosis. *Eur Respir J.* 2010;35:821–9.
12. Richeldi L, du Bois RM, Raghu G, Azuma A, Brown KK, Costabel U, et al. Efficacy and safety of nintedanib in idiopathic pulmonary fibrosis. *N Engl J Med.* 2014;370:2071–82.
13. Jiang C, Huang H, Liu J, Wang Y, Lu Z, Xu Z. Adverse events of pirfenidone for the treatment of pulmonary fibrosis: a meta-analysis of randomized controlled trials. *PLoS ONE.* 2012;7:e47024.
14. Micheletti R, Plaisance I, Abraham BJ, Sarre A, Ting CC, Alexanian M, et al. The long noncoding RNA Wisper controls cardiac fibrosis and remodeling. *Sci Transl Med* 2017;9:eaai9118.
15. Liu R, Li X, Zhu W, Wang Y, Zhao D, Wang X, et al. Cholangiocyte-derived exosomal long noncoding RNA H19 promotes hepatic stellate cell activation and cholestatic liver fibrosis. *Hepatology.* 2019;70:1317–35.
16. Feng M, Tang PM, Huang XR, Sun SF, You YK, Xiao J, et al. TGF- β mediates renal fibrosis via the Smad3-ErbB4-IR long noncoding RNA axis. *Mol Ther.* 2018;26:148–61.
17. Savary G, Dewaeles E, Diazi S, Buscot M, Nottet N, Fassy J, et al. The long noncoding RNA DNM3OS is a reservoir of FibromiRs with major functions in lung fibroblast response to TGF- β and pulmonary fibrosis. *Am J Respir Crit Care Med.* 2019;200:184–98.
18. Yan W, Wu Q, Yao W, Li Y, Liu Y, Yuan J, et al. MiR-503 modulates epithelial-mesenchymal transition in silica-induced pulmonary fibrosis by targeting PI3K p85 and is sponged by lncRNA MALAT1. *Sci Rep.* 2017;7:11313.
19. Liu H, Wang B, Zhang J, Zhang S, Wang Y, Zhang J, et al. A novel lnc-PCF promotes the proliferation of TGF- β 1-activated epithelial cells by targeting miR-344a-5p to regulate map3k11 in pulmonary fibrosis. *Cell Death Dis.* 2017;8:e3137.
20. Zhao X, Sun J, Chen Y, Su W, Shan H, Li Y, et al. lncRNA PFAR promotes lung fibroblast activation and fibrosis by targeting miR-138 to regulate the YAP1-Twist axis. *Mol Ther.* 2018;26:2206–17.
21. Sun J, Su W, Zhao X, Shan T, Jin T, Guo Y, et al. lncRNA PFAR contributes to fibrogenesis in lung fibroblasts through competitive binding to miR-15a. *Biosci Rep* 2019;39.
22. Hao K, Lei W, Wu H, Wu J, Yang Z, Yan S, et al. lncRNA-Safe contributes to cardiac fibrosis through Safe-Sfrp2-HuR complex in mouse myocardial infarction. *Theranostics.* 2019;9:7282–97.
23. Wang Y, Xu P, Zhang C, Feng J, Gong W, Ge S, et al. lncRNA NRON alleviates atrial fibrosis via promoting NFATc3 phosphorylation. *Mol Cell Biochem.* 2019;457:169–77.
24. Wang P, Luo ML, Song E, Zhou Z, Ma T, Wang J, et al. Long noncoding RNA lnc-TSI inhibits renal fibrogenesis by negatively regulating the TGF- β /Smad3 pathway. *Sci Transl Med* 2018;10:eaat2039.
25. Chen LL. Linking long noncoding RNA localization and function. *Trends Biochem Sci.* 2016;41:761–72.
26. Xing Y, Zhao X, Yu T, Liang D, Li J, Wei G, et al. MiasDB: a database of molecular interactions associated with alternative splicing of human pre-mRNAs. *PLoS ONE.* 2016;11:e0155443.
27. Shinde AV, Kelsh R, Peters JH, Sekiguchi K, Van De Water L, McKeown-Longo PJ. The α 4 β 1 integrin and the EDA domain of fibronectin regulate a profibrotic phenotype in dermal fibroblasts. *Matrix Biol.* 2015;41:26–35.
28. Klingberg F, Chau G, Walraven M, Boo S, Koehler A, Chow ML, et al. The fibronectin ED-A domain enhances recruitment of latent TGF- β -binding protein-1 to the fibroblast matrix. *J Cell Sci* 2018;131:jcs201293.
29. Li X, Yu T, Shan H, Jiang H, Sun J, Zhao X, et al. lncRNA PFAL promotes lung fibrosis through CTGF by competitively binding miR-18a. *FASEB J.* 2018;32:5285–97.
30. Jiang H, Chen Y, Yu T, Zhao X, Shan H, Sun J, et al. Inhibition of lncRNA PFRL prevents pulmonary fibrosis by disrupting the miR-26a/smad2 loop. *Am J Physiol Lung Cell Mol Physiol.* 2018;315:L563–L575.
31. Hsiao J, Yuan TY, Tsai MS, Lu CY, Lin YC, Lee ML, et al. Upregulation of haploinsufficient gene expression in the brain by targeting a long non-coding RNA improves seizure phenotype in a model of Dravet syndrome. *EBioMedicine.* 2016;9:257–77.
32. Khalil AM, Guttman M, Huarte M, Garber M, Raj A, Rivea Morales D, et al. Many human large intergenic noncoding RNAs associate with chromatin-modifying complexes and affect gene expression. *Proc Natl Acad Sci USA.* 2009;106:11667–72.
33. Subramanian RR, Wusk MA, Ogilvie KM, Bhat A, Kuang B, Rockel TD, et al. Enhancing antisense efficacy with multimers and multi-targeting oligonucleotides (MTOs) using cleavable linkers. *Nucleic Acids Res.* 2015;43:9123–32.
34. Sokół E, Bogusławska J, Piekietko-Witkowska A. The role of SRSF1 in cancer. *Postepy Hig i Med doswiadczalnej (Online).* 2017;71:422–30.
35. Zhou X, Wang R, Li X, Yu L, Hua D, Sun C, et al. Splicing factor SRSF1 promotes gliomagenesis via oncogenic splice-switching of MYO1B. *J Clin Investig.* 2019;129:676–93.
36. Comiskey DF Jr., Jacob AG, Singh RK, Tapia-Santos AS, Chandler DS. Splicing factor SRSF1 negatively regulates alternative splicing of MDM2 under damage. *Nucleic Acids Res.* 2015;43:4202–18.
37. Anczuków O, Rosenberg AZ, Akerman M, Das S, Zhan L, Karni R, et al. The splicing factor SRSF1 regulates apoptosis and proliferation to promote mammary epithelial cell transformation. *Nat Struct Mol Biol.* 2012;19:220–8.
38. Cramer P, Cáceres JF, Cazalla D, Kadener S, Muro AF, Baralle FE, et al. Coupling of transcription with alternative splicing: RNA pol II promoters modulate SF2/ASF and 9G8 effects on an exonic splicing enhancer. *Mol Cell.* 1999;4:251–8.
39. Lopez-Mejia IC, De Toledo M, Della Seta F, Fafet P, Rebouissou C, Deleuze V, et al. Tissue-specific and SRSF1-dependent splicing of fibronectin, a matrix protein that controls host cell invasion. *Mol Biol Cell.* 2013;24:3164–76.